

Supporting information for

HgTe Nanocrystals for SWIR Detection and their Integration up to Focal Plane Array

Audrey Chu^{1,2}, Bertille Martinez^{1,3}, Simon Ferre⁴, Vincent Noguier⁴, Charlie Gréboval¹, Clément Livache^{1,3}, Junling Qu¹, Yoann Prado¹, Nicolas Casaretto¹, Nicolas Goubet^{4,5}, Hervé Cruguel¹, Lenart Dudy⁶, Mathieu G. Silly⁶, Grégory Vincent², Emmanuel Lhuillier^{1*}

¹Sorbonne Université, CNRS, Institut des NanoSciences de Paris, INSP, F-75005 Paris, France

²ONERA-The French Aerospace Lab, Chemin de la Hunière, BP 80100, F-91123 Palaiseau, France

³Laboratoire de Physique et d'Étude des Matériaux, ESPCI Paris PSL Research University, Sorbonne Université Univ Paris 06, CNRS, 10 rue Vauquelin 75005 Paris, France.

⁴New Imaging Technologies SA, 1 impasse de la Noisette 91370 Verrières le Buisson, France

⁵Sorbonne Université, CNRS, De la Molécule aux Nano-objets: Réactivité, Interactions et Spectroscopies, MONARIS, F-75005 Paris, France

⁶Synchrotron-SOLEIL, Saint-Aubin, BP48, F91192 Gif sur Yvette Cedex, France

*To whom correspondence should be sent: el@insp.upmc.fr

Table of content

1. Material characterization	3
1.1. Electronic microscopy.....	3
1.2. X-ray diffraction.....	3
1.3. Optical characterization	3
1.4. X Ray Photoemission	4
1.5. UV Photoelectron Spectroscopy.....	5
2. Transport and phototransport measurements	7
2.1. Device fabrication.....	7
2.2. Electrical Measurements.	7
2.3. Device performances.....	8
2.4. Pixel Matrix.....	9
2.5. Deposition on read out circuit.....	10
3. Temperature dependence of nanocrystal films	12
4. References.....	12

1. Material characterization

1.1. Electronic microscopy

For Transmission electronic microscopy (TEM) pictures, a drop of CQD solution is drop-cast on a copper grid covered with an amorphous carbon film. JEOL 2010F is used at 200 kV for acquisition of picture. For device characterization, a FEI Magellan scanning electron microscope is used.

For scanning electronic microscopy (SEM) pictures, FEI Magellan scanning electron microscope is used. The current of the beam is adjusted to 6 pA and the operating bias is set to 3 kV.

1.2. X-ray diffraction

X ray diffraction is conducted by dropcasting a solution of CQDs on a Si wafer. The diffractometer is a Rigaku Smartlab based on the emission of the Cu K_{α} line. X-ray diffraction of the two materials reveals a zinc blende phase for HgTe^{1,2} and a rock slat phase for PbS³, see Figure S 1

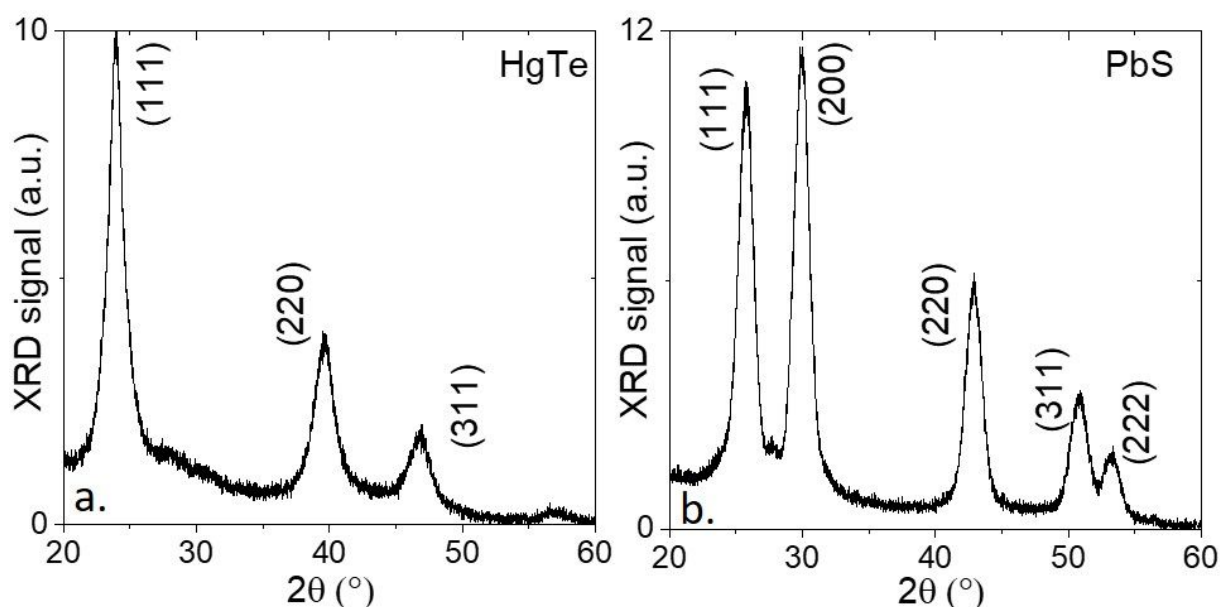


Figure S 1 x-ray diffractogram from HgTe (a.) and PbS (b.) CQD with a band edge at 6000 cm^{-1} .

1.3. Optical characterization

Sample preparation for infrared spectroscopy. A glass slide is cut in $15 \times 15\text{ mm}^2$ pieces. Those substrates are rinsed with acetone and sonicated in acetone for 5 minutes. They are then rinsed with acetone and isopropanol and dried with a N_2 gun. A solution of CQDs at $30\text{ mg}\cdot\text{mL}^{-1}$ in toluene is spin-coated on those substrates (2000 rpm, 60 s). Afterwards, the ligand exchange procedure is carried out by dipping the film in the solution containing the new ligands for 60 s and rinsed in EtOH for 30 s. All ligand exchange solutions are prepared at 1 w% in ethanol except NH_4Cl , for which the solvent is MeOH. This process is repeated at least 2 to 3 times to build thick films.

Infrared spectroscopy is conducted using a Fisher IS50 Fourier transform Infrared spectrometer. The visible light source is used and shone on CaF_2 beam splitter. To measure film absorption, an extended

InGaAs detector is used. Each spectrum is averaged 32 times and the resolution is set to 4 cm^{-1} . Photocurrent spectrum are acquired as the sample is biased using a Femto DLPCA current amplifier which role is also to magnify the current. The signal is then fed into the FTIR acquisition board.

Analysis of surface chemistry (Figure 1b): We observe the interband edge transition around 6000 cm^{-1} . In addition, we observe a clear strong contribution from the C-H bond at 2900 cm^{-1} relative to the ligand. There is a small peak from CO_2 due to in air measurement. For PbS, we also observe a clear strong contribution from C=O bond due to the presence of oleate.

1.4. X Ray Photoemission

Sample for XPS or UPS. Silicon wafer were rinsed with acetone, sonicated in acetone for 5 minutes. They were rinsed again with acetone and isopropanol and dried with N_2 gun. A 5 nm layer of Cr and an 80 nm layer of Au were deposited using thermal evaporation. A thin layer (≈ 50 nm) of QDs was deposited on those substrates using the same procedure described for photoconductive device preparation. Ligand exchange is conducted according to the same procedure. All ligand exchange solutions are prepared at 1 wt % in ethanol except NH_4Cl , for which the solvent is MeOH.

The film is then introduced in the preparation chamber, degassed for at least an hour and transferred to the analysis chamber. The measurements were conducted at 600 eV. This photon energy is precisely measured using the first and second order of 4f core level of Au using the formula: $h\nu_{exp} = KE_{2^{nd}} - KE_{1^{st}}$.

The work function of the analyzer (WF_A) is determined by measuring the kinetic energy of electrons at the Fermi level for the gold (set to 0 eV). $WF_A = h\nu_{exp} - KE_{Fermi}$

For the measurement of the secondary electron cut-off, the sample is biased with an 18 V battery. The exact bias is determined by measuring the shift of the 4f core level of the gold when the bias is applied.

XPS overview. The overview is acquired with a 50 eV pass energy and a 0.5 eV resolution. The obtained spectra for PbS and HgTe are given in Figure S 2.

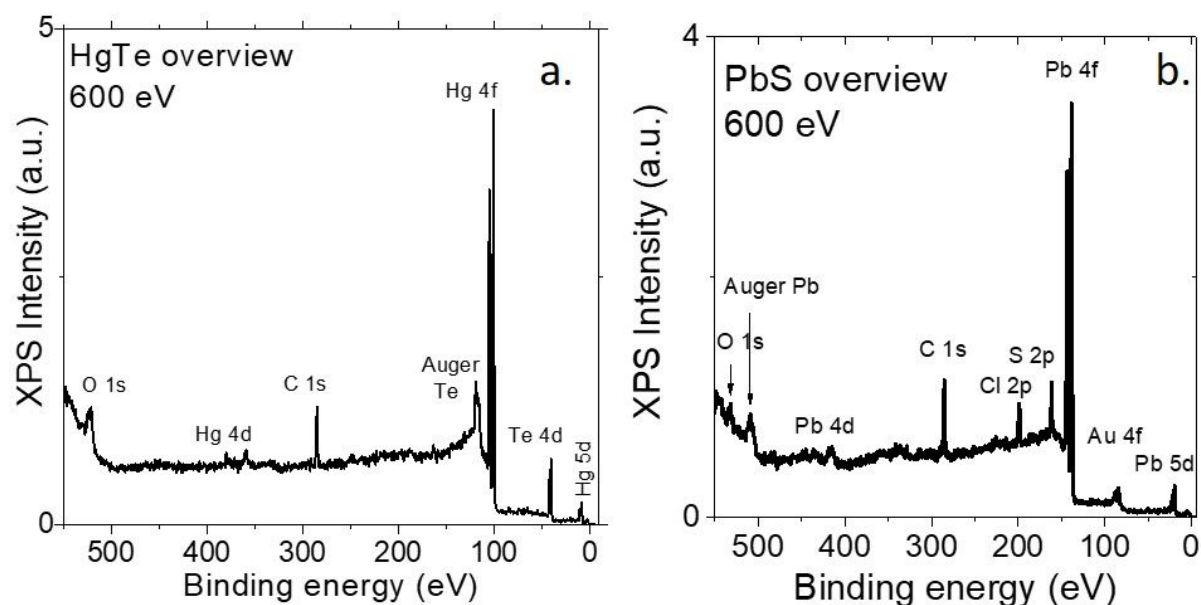


Figure S 2: XPS overview for a thin film of HgTe (a) or PbS (b) capped with EDT.

In the case of HgTe we only observe contribution of Hg, Te and from the ligands (C). A very limited O contribution is observed due to air preparation, see Figure S 2a.

For PbS, We notice contributions of Pb and S, as well carbon and residual Cl from the PbCl₂ precursor, see Figure S 2b.

Valence band measurement. We determine the value of VB-E_F looking at high KE electrons. We measure the highest kinetic energy available (KE_{VB}) and extract VB-E_F with the formula: $VB - E_F = h\nu_{exp} - KE_{VB} - WF_A$.

Work function measurement. In order to measure the work function, which is the difference in energy between vacuum level and Fermi level, we look for the cut off of secondary electrons (KE_{cut off}). We start by polarizing the sample using an 18 V (Pol_{bias}) battery and look for the low kinetic energy electrons. The work function is deduced with the formula: $WF_{Sample} = KE_{Cut\ off} - Pol_{Bias}$.

1.5. UV Photoelectron Spectroscopy

The film is introduced in the preparation chamber and degassed for at least an hour and transferred to the analysis chamber. The measurements were conducted using a helium lamp. The photon energy is 21.21 eV.

The work function of the analyzer (WF_A) is determined by measuring the kinetic energy of electrons at the fermi level for the gold (set to 0 eV). $WF_A = h\nu_{exp} - KE_{Fermi}$

For the measurement of the secondary electron cut-off, the sample is biased with an 18 V battery. The exact bias is determined by measuring the shift of the 4f core level of the gold when the bias is applied.

Valence band measurement. We determine the value of VB-E_F looking at high KE electrons. We measure the highest kinetic energy available (KE_{VB}) and extract VB-E_F with the formula: $VB - E_F = h\nu_{exp} - KE_{VB} - WF_A$.

Work function measurement. In order to measure the work function, which is the difference in energy between vacuum level and Fermi level, we look for the cut off of secondary electrons. We start by polarizing the sample using an 18 V battery and look for the low kinetic energy electrons. The work function is deduced with the formula: $WF_{Sample} = KE_{Cut\ off} - Pol_{Bias}$.

Figure S 3 shows the valence band and the secondary electron cut off for thin film of HgTe nanocrystals capped with various ligands.

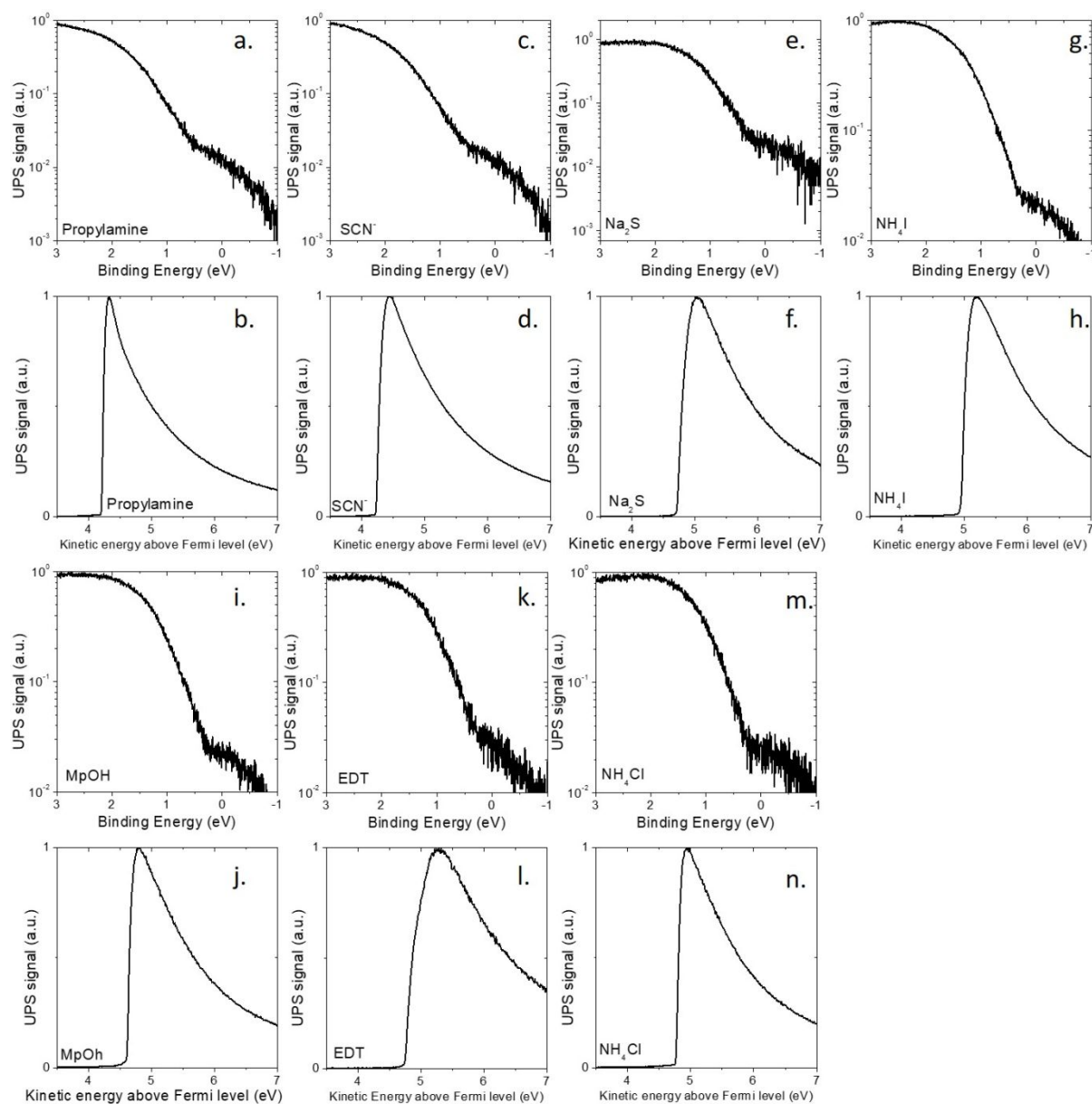


Figure S 3: Valence band signal as a function of the electron binding energy for a thin film of HgTe CQDs capped with propylamine (a), SCN^- (c), S^{2-} (e), I^- (g), MPOH (i), EDT (k) et Cl (m). Secondary electron cut-off as a function of the (re-calibrated) electron kinetic energy for a thin film of HgTe CQDs capped with propylamine (b), SCN^- (d), S^{2-} (f), I^- (h), MPOH (j), EDT (l) et Cl (n). The sample is polarized with an 18 V battery.

2. Transport and phototransport measurements

2.1. Device fabrication

Electrolyte gating. In a N_2 glovebox, 0.5 g of $LiClO_4$ and 2.3 g of PEG are mixed in a vial. This vial is heated at 170 °C on a hot plate for 2 h until the solution becomes clear. To use the electrolyte, the solution is warmed up around 100 °C and brushed onto the CQD film.

Si/SiO₂/Au Electrodes. The surface of Si/SiO₂ wafer (400 nm oxide layer) is cleaned by sonication in acetone. The wafer is rinsed with acetone, then isopropanol and dried with a N_2 gun. A final cleaning is made using an O₂ plasma. An adhesion primer (TI PRIME) is spin-coated onto the substrate and baked at 120 °C for 2 min. AZ5214E is spin-coated and baked at 110 °C for 90 s. The substrate is exposed under UV through a pattern mask for 1.5 s. The film is then baked at 125 °C for 2 min in order to invert the resist. Then a 40 s flood exposure is performed. The resist is developed using a bath of AZ726 for 32 s and rinsed in pure water and dried with N_2 . We then deposit 5 nm of chromium layer and 80 nm of gold layer using thermal evaporation. The lift-off is performed by dipping the film in acetone for 1 hour. The electrodes are rinsed using isopropanol and dried using a N_2 gun. The electrodes are 2.5 mm long spaced by 20 μ m. These electrodes are used for photoconductive devices and electrolyte-gated transistor measurements. A scheme of the transistor is given in Figure S 4.

Photoconductive Device preparation. The solvent of CQD solution is changed for hexane-octane (9:1). Inside a N_2 filled glovebox, CQD in hexane-octane is drop-casted on prepatterned interdigitated gold electrodes. After a complete drying, EDT ligand exchange is performed by dipping the film in an EDT solution in ethanol (1 wt %) for 90 s and rinsing it in pure ethanol for 30 s. This process is repeated for 5-7 times to get homogeneous and crack free film with a device resistance of 1-2 M Ω .

2.2. Electrical Measurements.

DC Transport. The sample is connected to a Keithley 2634b, which controls the drain bias (V_{DS}) and measures the associated current (I_{DS}). This measure is carried out in the dark or under illumination using a 1.55 μ m diode.

Transistor Measurement. The sample is connected to a Keithley 2634b, which sets the drain source bias (V_{DS}), controls the gate bias (V_{GS}) with a step of 1 mV and measures the associated currents (I_{DS} and I_{GS}).

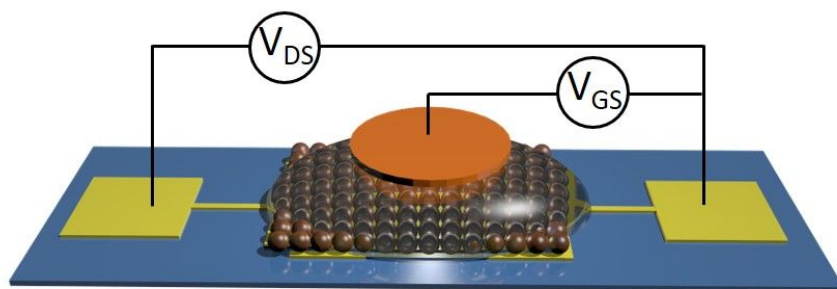


Figure S 4 : Scheme of an electrolyte transistor.

2.3. Device performances

We have characterized the devices performances for both PbS and HgTe, see Figure S 5 and Figure S 6 respectively. The detectivity is low for both materials: 2.6×10^7 Jones for PbS and 1.2×10^7 for HgTe.

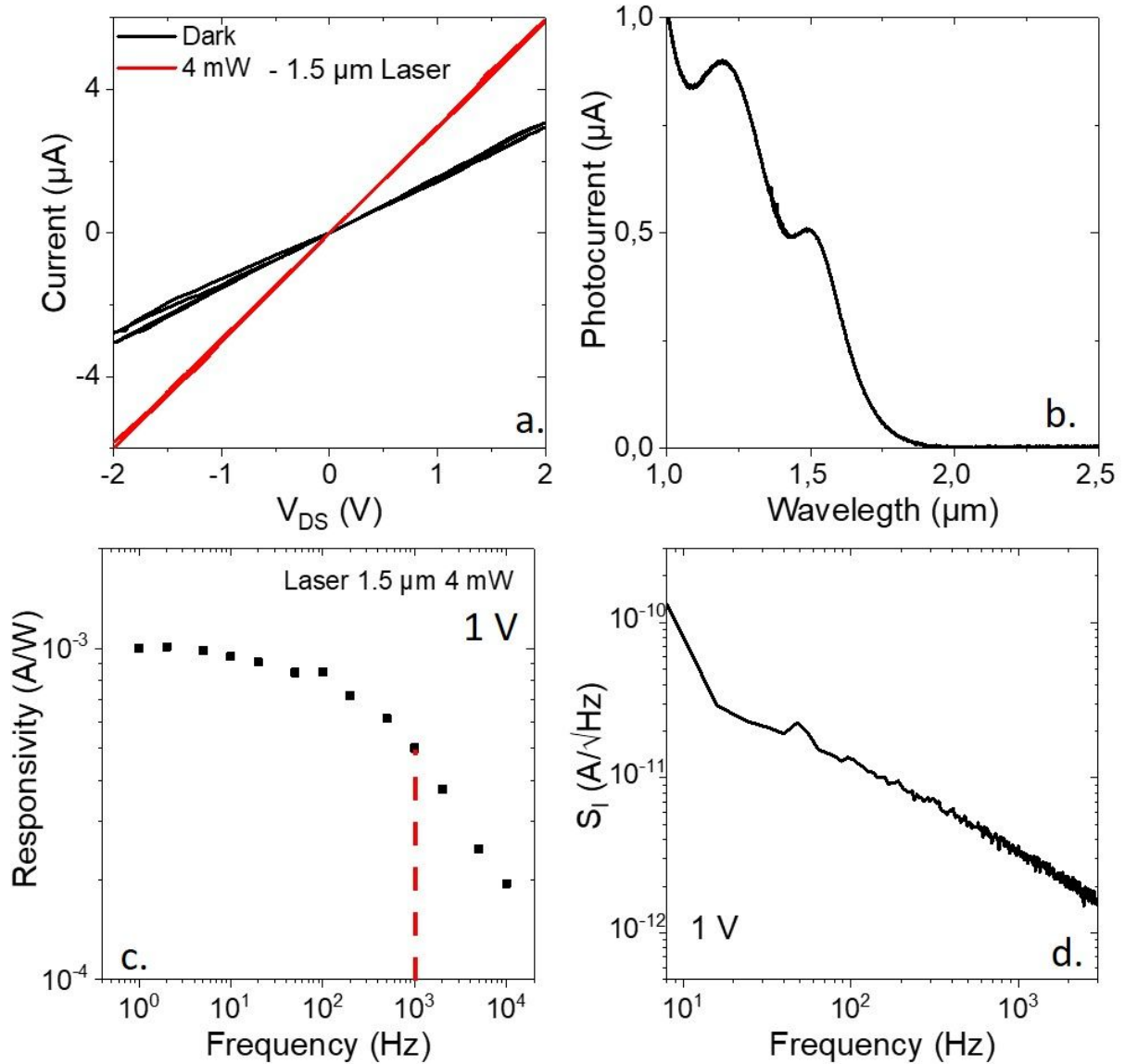


Figure S 5 **PbS nanocrystals on interdigitated electrode** : a. I-V curves under dark condition and under illumination ($\lambda=1.55 \mu\text{m}$) measured at room temperature. b. Photocurrent spectra of the device. c. Responsivity at 1 V as a function of the signal frequency. d. Noise current spectral density as a function of the signal frequency.

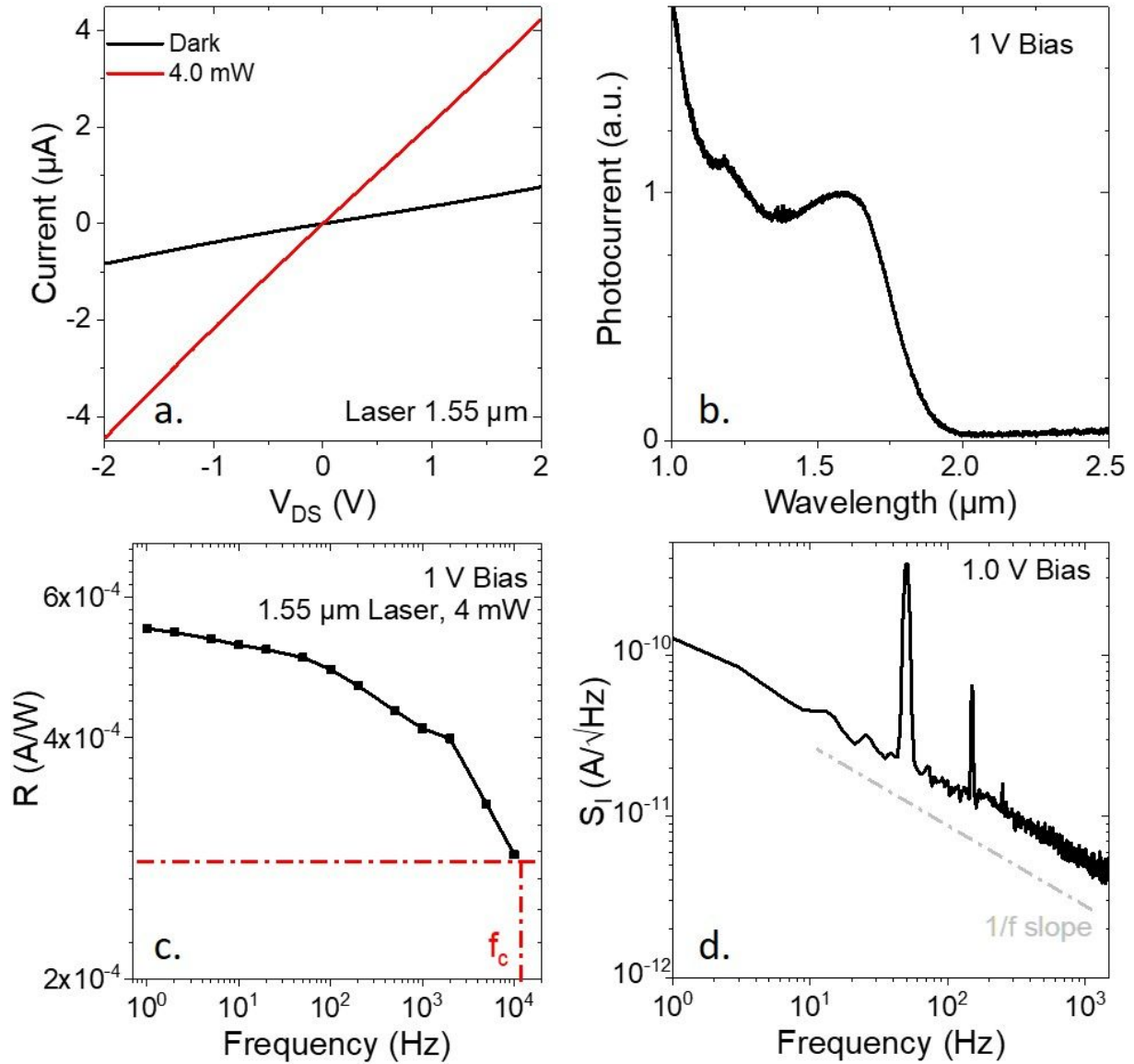


Figure S 6 **HgTe nanocrystals on interdigitated electrode** : a. I-V curves under dark condition and under illumination ($\lambda=1.55 \mu\text{m}$) measured at room. b. Photocurrent spectra of the device. c. Responsivity at 1 V as a function of the signal frequency. d. Noise current spectral density as a function of the signal frequency.

2.4. Pixel Matrix

The fabrication of the array of pixel is taken from Martinez *et al.*⁴ The matrix of pixel is made of 10×10 pixels with a $30 \mu\text{m}$ size.

Electrode preparation. Step 1: A half microscope slide is washed with acetone, sonicated in an acetone bath for 4 min and then rinsed using acetone and isopropanol. It is then dried with N_2 and plasma-cleaned for 5 min. Adhesion promoter (TI-PRIME) is spin coated on the substrate (4000 rpm, 1000

rpm/s, 30s) and then annealed at 120 °C for 2 min. The photosensitive resist (AZ 5214E) is then spin coated on the substrate (4000 rpm, 1000 rpm/s, 30 s) and then annealed at 110 °C for 90 s. The sample is then exposed to UV through a first pattern chromium mask for 1.5 s. The resist is inverted by an annealing step (125 °C, 2 min) and then a 40 s flood exposure is performed. The sample is developed in AZ 726 between 16 and 25 s and then rinsed in pure water. The patterned sample can then be plasma-cleaned again for 5 min before being put in a VINCI evaporator for a 5 nm of Cr and a 40 nm of gold depositions. At the end of evaporation, the sample is dipped in acetone overnight to remove the remaining resist. **Step 2:** The sample is washed with acetone and isopropanol before being dried with N₂. The depositions of TI-PRIME and AZ 5214E resist follow the same procedure as described in step 1. The sample is then insolated through a second pattern chromium mask for 8 s. This time, the lithography is positive so the resist is neither inverted with an annealing step neither re-exposed to UV for flood exposure. The sample is directly developed using AZ 726 developer for 45 s before being rinsed in pure water. The patterned sample is then put in an Alcatel sputtering chamber for a 27 min deposition of SiO_x, at 120 W. At the end of sputtering, the sample is dipped in acetone overnight to remove remaining resist, and finally sonicated at low power to gently remove the resist which is sticking on the substrate. The obtained SiO_x layer is 75 nm thick. **Step 3:** After having rinsed the sample with acetone and isopropanol, the adhesion promoter and the resist are deposited as described in steps 2 and 3. The sample is then exposed through a third chromium mask for 1.5 s. The same resist inversion process as described in step 1 (annealing + flood exposure) is performed before developing the sample in AZ 726 developer for 16 s and rinsing it in pure water. The patterned sample is then put in a VINCI evaporator for a 5 nm Cr and a 150 nm Au depositions. At the end, the sample is dipped in acetone overnight to remove remaining resist.

Ink preparation. 30 mg of Na₂S are dissolved in 10 mL of DMF. 0.5 mL of this short-ligand solution is added to 0.5 mL of a HgTe solution at 50 mg.mL⁻¹ in toluene. A few mL of hexane can be added to help phase dissociation: the QDs migrate to the bottom phase (DMF), showing efficient ligand exchange. After 3 washing steps with hexane, the QDs are centrifuged at 6000 rpm for 5 min. The clear supernatant is discarded and the QDs are redispersed in 250 µL of fresh DMF to reach a concentration of 100 mg.mL⁻¹. To remove all instable phase in the solution, it is centrifugated at 3000 rpm for 3 minutes. The supernatant is the ink that we use. The ink is used immediately after preparation.

Ink deposition. The ink is deposited onto of the pixel matrix using spin-coating at 2000 rpm for 1 minute. Seven layers are deposited to make the film.

2.5. Deposition on read out circuit

Ink preparation. 5 mg of HgCl₂, 100 µL of MPOH and 900 µL of DMF are mixed. 0.5 mL of this solution is added to 0.5 mL of a HgTe solution at 50 mg.mL⁻¹ in toluene. A few mL of hexane can be added to help phase dissociation: the QDs migrate to the bottom phase (DMF), showing efficient ligand exchange. QDs are centrifuged at 6000 rpm for 10 min. The clear supernatant is discarded and the QDs are redispersed in DMF to reach a concentration of 300 mg.mL⁻¹. To ensure that the colloidal stability

is good, the sample is then re-centrifuged at 3000 rpm for 4 min. If the ligand exchange is successful, no QDs should have fallen at the bottom of the tube at the end of centrifugation.

Ink deposition. The ink is deposited onto the read-out circuit using a two-steps spin-coating process: 1) at 600 rpm ($400 \text{ rpm}\cdot\text{s}^{-1}$) for 180 s and 2) at 3000 rpm ($1000 \text{ rpm}\cdot\text{s}^{-1}$) for 30 s. The film is then dried for at least 2 hours under primary vacuum.

3. Temperature dependence of nanocrystal films

Optical and electrical properties of an HgTe film annealed for 15 minutes at different temperature (50°C, 100°C and 150°C) are very similar if the baking is made under ambient atmosphere (Air) or under inert conditions in a N₂ glovebox, see Figure S 7. However, for PbS CQD film, the annealing under inert conditions is quite different than the one under air. First no blue shift is observed at 50 °C. Secondly at 150°C the optical feature is completely lost to obtain a long tail of absorption. Finally, the dark current is dramatically increased with annealing step under inert condition while it was stable under ambient condition. All those observations are consistent with the formation of a shell of PbO with an annealing in air.

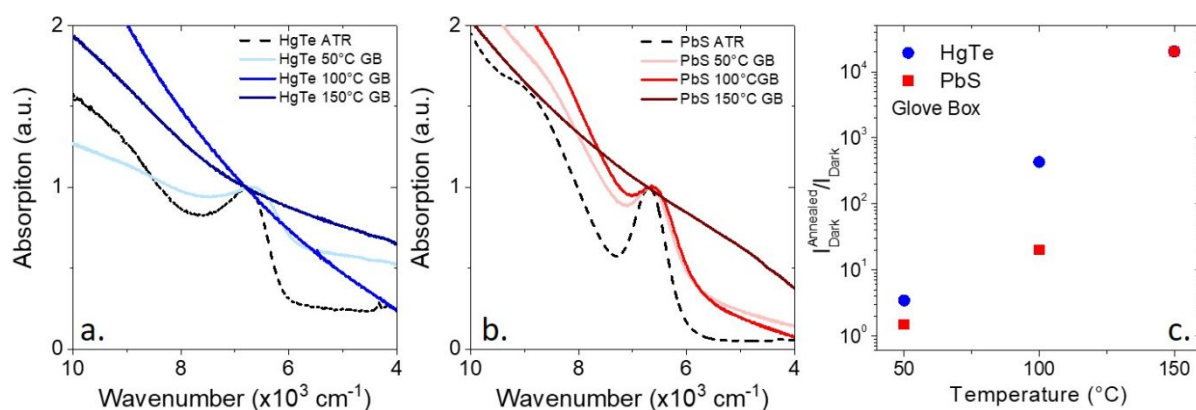


Figure S 7: a. Absorption of HgTe nanocrystals thin film in solution and under thin film form after annealing at various temperature in glove box. b. Absorption of PbS nanocrystals thin film in solution and under thin film form after annealing at various temperature in glove box. c. Ratio of the current after and before annealing for thin film of HgTe and PbS nanocrystal as a function of the annealing temperature. The annealing is made in a N₂ filled glovebox.

4. References

- (1) Keuleyan, S.; Lhuillier, E.; Guyot-Sionnest, P. Synthesis of Colloidal HgTe Quantum Dots for Narrow Mid-IR Emission and Detection. *J. Am. Chem. Soc.* **2011**, *133*, 16422–16424.
- (2) Kovalenko, M. V.; Kaufmann, E.; Pachinger, D.; Roither, J.; Huber, M.; Stangl, J.; Hesser, G.; Schäffler, F.; Heiss, W. Colloidal HgTe Nanocrystals with Widely Tunable Narrow Band Gap Energies: From Telecommunications to Molecular Vibrations. *J. Am. Chem. Soc.* **2006**, *128*, 3516–3517.
- (3) Moreels, I.; Lambert, K.; Smeets, D.; De Muynck, D.; Nollet, T.; Martins, J. C.; Vanhaecke, F.; Vantomme, A.; Delerue, C.; Allan, G.; et al. Size-Dependent Optical Properties of Colloidal PbS Quantum Dots. *ACS Nano* **2009**, *3*, 3023–3030.
- (4) Martinez, B.; Ramade, J.; Livache, C.; Goubet, N.; Chu, A.; Gréboval, C.; Qu, J.; Watkins, W. L.; Becerra, L.; Dandeu, E.; et al. HgTe Nanocrystal Inks for Extended Short-Wave Infrared Detection. *Advanced Optical Materials* **2019**, 1900348.